J. Biochem. 2011;150(5):579–591 doi:10.1093/jb/mvr100

JB THE JOURNAL OF BIOCHEMISTRY

A molecular design that stabilizes active state in bacterial allosteric L-lactate dehydrogenases

Received May 26, 2011; accepted July 18, 2011; published online August 9, 2011

Kazuhito Arai[1], Jun Ichikawa[1], Shinta Nonaka[1], Akimasa Miyanaga[1], Hiroyuki Uchikoba[2], Shinya Fushinobu[2] and Hayao Taguchi[1,*]

[1]Department of Applied Biological Science, Faculty of Science and Technology, Tokyo University of Science, 2641 Yamazaki, Noda, Chiba 278-8510 and [2]Department of Biotechnology, The University of Tokyo, 1-1-1 Yayoi, Bunkyo-ku, Tokyo 113-8657, Japan

*Hayao Taguchi, Department of Applied Biological Science, Faculty of Science and Technology, Tokyo University of Science, 2641 Yamazaki, Noda, Chiba 278-8510, Japan. Tel: +81-4-7122-9414, Fax: +81-4-7123-9767, email: htaguchi@rs.noda.tus.ac.jp

L-Lactate dehydrogenase (L-LDH) of *Lactobacillus casei* (LCLDH) is a typical bacterial allosteric L-LDH that requires fructose 1,6-bisphosphate (FBP) for its enzyme activity. A mutant LCLDH was designed to introduce an inter-subunit salt bridge network at the *Q*-axis subunit interface, mimicking *Lactobacillus pentosus* non-allosteric L-LDH (LPLDH). The mutant LCLDH exhibited high catalytic activity with hyperbolic pyruvate saturation curves independently of FBP, and virtually the equivalent K_m and V_m values at pH 5.0 to those of the fully activated wild-type enzyme with FBP, although the K_m value was slightly improved with FBP or Mn^{2+} at pH 7.0. The mutant enzyme exhibited a markedly higher apparent denaturating temperature ($T_{1/2}$) than the wild-type enzyme in the presence of FBP, but showed an even lower $T_{1/2}$ without FBP, where it exhibited higher activation enthalpy of inactivation ($\Delta H^{\ddagger}$). This result is consistent with the fact that the active state is more unstable than the inactive state in allosteric equilibrium of LCLDH. The LPLDH-like network appears to be conserved in many bacterial non-allosteric L-LDHs and dimeric L-malate dehydrogenases, and thus to be a key for the functional divergence of bacterial L-LDHs during evolution.

Keywords: allosteric regulation/bacteria/catalysis/glycolysis/site-directed mutagenesis.

Abbreviations: BLLDH, *Bifidobacterium longum* L-LDH; BSLDH, *Bacillus stearothermophilus* L-LDH; FBP, fructose 1,6-bisphosphate; LCLDH, *Lactobacillus casei* L-LDH; L-LDH, L-lactate dehydrogenase; LPLDH, *Lactobacillus pentosus* L-LDH; NADH, nicotinamide adenine dinucleotide; TCLDH, *Thermus caldophilus* L-LDH.

L-Lactate dehydrogenase (L-LDH; EC 1.1.1.27) catalyses the reduction of pyruvate to L-lactate with the oxidation of NADH to NAD^+, and plays a key role in the last step of anaerobic glycolysis and L-lactate fermentation (*1*). L-LDH is a highly divergent enzyme in primary structure and catalytic properties, depending on the organism or tissue. Many bacteria possess allosteric types of L-LDH, including extreme thermophiles such as *Thermus* (*2–5*) and *Thermotoga* (*6*) species, whereas vertebrates have non-allosteric types of isozymes. For the bacterial allosteric enzymes, fructose 1,6-bisphosphate (FBP) commonly induces high catalytic activity mostly through drastic improvement of substrate binding, though such FBP requirement is undesirable for the industrial or experimental application of L-LDHs. In the absence of FBP, many of the enzymes exhibit sigmoidal shaped substrate saturation curves, or no enzyme activity with conventional pyruvate concentrations, and less frequently some enzymes such as *Bacillus stearothermophilus* L-LDH (BSLDH) (*7*) show a hyperbolic substrate saturation curve with much larger substrate K_m values. It nevertheless remains unclear which key structural feature endows L-LDHs with an allosteric or non-allosteric property.

The allosteric regulation of L-LDHs has been extensively studied for the allosteric enzymes of *Thermus caldophilus* (TCLDH) (*8–12*), *Bacillus stearothermophilus* (BSLDH) (*13–18*), *Bifidobacterium longum* (BLLDH) (*19–22*) and *Lactobacillus casei* (LCLDH) (*23–30*), all of which comprise four identical subunits that are related through three 2-fold axes, the P, Q and R axes, as in the case of the vertebrate enzymes (Fig. 1A). The inactive and active state structures of liganded BLLDH (*20*) and unliganded LCLDH (*30*) consistently indicate that the two states coexist in allosteric equilibrium independently of allosteric ligands, as described by Monod *et al.* (*31*). The two enzymes commonly undergo a great quaternary structural change between the inactive (T) and active (R) state structures, in which the P-axis-related dimers take on open and closed conformations, respectively (Fig. 1A), although BSLDH is dissociated into the inactive *Q*-axis-related dimer, which exhibits a low substrate affinity (large K_m), at a physiological protein concentration in the absence of FBP (*13*, *14*, *18*).

Known allosteric L-LDHs have two FBP binding sites per tetramer at the P-axis subunit interface, which correspond to the anion-binding site of the vertebrate enzymes (*32*) and four catalytic sites near the *Q*-axis subunit interface in the tetramer (Fig. 1A) (*17*, *20*), as in the case of the vertebrate enzymes. In each catalytic site, only one subunit contains all known important amino acids for catalysis, but the *Q*-axis-related subunit appears to indirectly participate in the formation of the catalytic site structure through inter-subunit interactions (Fig. 1B). The BLLDH and

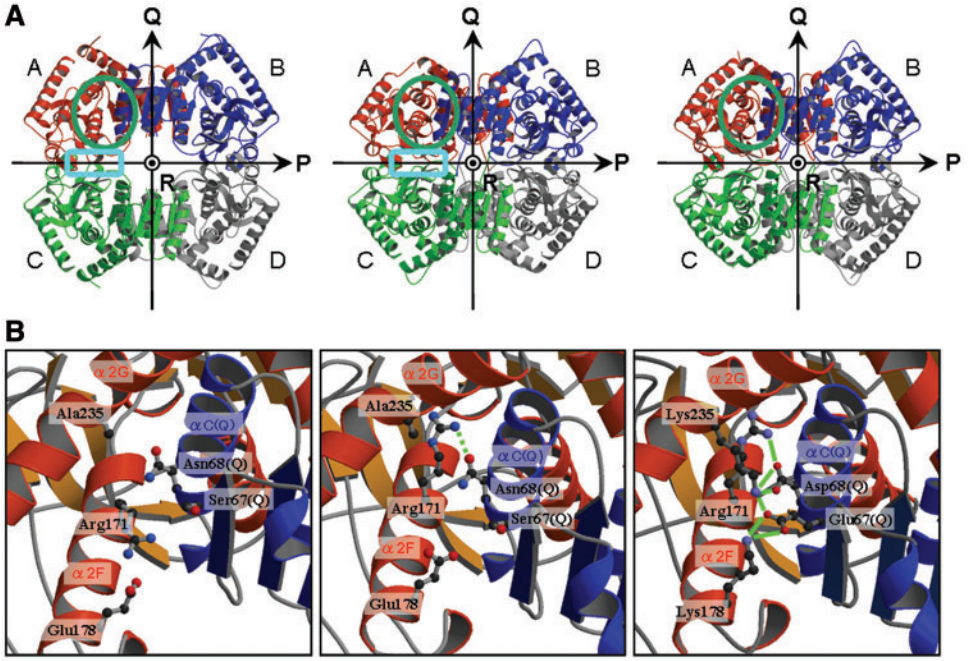

Fig. 1 Structural comparison of non-allosteric LPLDH, and the active (R) and inactive (T) states of LCLDH. (A) Ribbon diagrams of the tetrameric structures of the T (left) and R (middle) states of LCLDH and LPLDH (right), viewed along the molecular *R*-axis. The four subunits are coloured red, green, blue and grey in the three structures. The P and *Q*-axes, and *R*-axis are indicated by arrows and a circle, respectively. The approximate regions shown in (B) and FBP binding sites are encircled in green and cyan, respectively. (B) The regions around Arg171 where LPLDH forms unique inter-subunit salt bridges at the *Q*-axis subunit interface. The structures of the T (left) and R (middle) states of LCLDH and LPLDH (right) are represented by ribbon diagrams, where only the amino acids at positions 67, 68, 171, 178 and 235 are indicated by a ball and stick model. The two *Q*-axis-related subunits are coloured red and blue as in the case of (A). Salt bridges and hydrogen bonds among these amino acids are indicated by green solid and broken lines, respectively. The figures were drawn using MOLSCRIPT (*62*) and Raster3D (*63*).

LCLDH structures consistently indicate that structural rearrangements of the catalytic site are mostly concerned in switching of the orientation of Arg171 in the α2F helix (Fig. 1B, left and middle) (*20*, *30*) which plays a pivotal role in anchoring the substrate to the catalytic site through its bifurcated salt bridge with the substrate carboxyl group (*1*, *33*). The switching of Arg171 occurs through a sliding motion of the α2F helix on the αC helix of the Q-axis-related subunit [αC(Q)], and thereby highly depends on the flexibility of this contact area.

It is notable that the *Lactobaccilus pentosus* enzyme (LPLDH), which constitutively exhibits high catalytic activity independently of FBP in spite of its particularly high amino acid sequence identity (66%) with LCLDH (*34*), possesses a unique inter-subunit salt bridge network in the α2F–αC(Q) contact area, where basic residues, Arg171 and Lys178, in the α2F helix, and Lys235, in the α2G helix, form multiple inter-subunit salt bridges with acidic residues, Asp67 and Glu68, in the αC helix of the counterpart subunit (Fig. 1B, right) (*35*). This salt bridge network appears to tightly lock the α2F and αC(Q) helices together, with the orientation of Arg171. To determine the actual role of this salt bridge network, we replaced Ser67, Asn68, Glu178 and Ala235 of LCLDH by Glu, Asp, Lys and Lys, respectively, mimicking the salt bridge network of LPLDH. Concomitantly, Asp234 was replaced with Asn, since it may disturb the network with its negatively charged side chain. In this article, we describe the properties of the mutant LCLDH with these five amino acid replacements (Q5 mutant LCLDH).

Materials and Methods

Amino acid replacement and enzyme preparation

Site-directed mutagenesis was performed with a Quik-Change in vitro mutagenesis kit (Stratagene, La Jolla, CA, USA) to construct the gene of the Q5 mutant LCLDH, in which Ser67, Asn68, Glu178, Asp234 and Ala235 were replaced by Glu, Asp, Lys, Asn and Lys, respectively. The following primers and their complementary primers were purchased from Takara Syuzo (Kyoto, Japan), and used for site-directed mutagenesis: S67E/N68D, 5′-GAC GCG ATT GAC CTC GAG GAC GCG CTG CCA TTC-3′; E178K, 5′-TTC CGT CAG TCC ATC GCG AAA ATG GTT AAC GTT G-3′; and D234N/A235K, 5′-TTT GAA GAC GTT CGA AAC AAA GCA TAT GAA ATC-3′. The wild-type and mutant recombinant LCLDHs were expressed in *Escherichia coli* MV1184 cells, and purified essentially according to previous reports (*28*, *29*).

Enzyme assay and protein determination

Assaying of the purified enzymes was carried out at 30°C in 50 mM sodium acetate buffer (pH 5.0) or 50 mM sodium MOPS (morpholinopropanesulfonic acid) buffer (pH 7.0) containing 0.1 mM NADH, which is a saturating concentration for LCLDH. One unit was defined as the rate of the conversion of 1 μmol of substrate per min. Protein concentrations were determined by the Bradford method (*36*) with Bio-Rad Protein Assay protein reagent (Bio-Rad), using bovine serum albumin as a standard protein. The data that indicated significant substrate inhibition were interpreted

using an equation for substrate inhibition, according to Eszes *et al.* (*37*).

$$\frac{v}{V_m} = \frac{[S]}{[S] + K_m + [S]^2/K_I}$$

where v is the reaction velocity, V_m the maximal velocity, [S] the substrate concentration and K_I the inhibition constant for the substrate. In the case of data showing significant cooperative effects of ligand, the following Hill equation (*38*) was used for sigmoidal curve fitting.

$$\frac{v - V_0}{V_m} = \frac{[\text{ligand}]^{nH}}{[\text{ligand}]^{nH} + S_{0.5}^{nH}}$$

where V_0 is the reaction velocity with no ligand, (ligand) the concentration of ligand, such as pyruvate, FBP or Mn^{2+}, $S_{0.5}$ the half-saturating concentration of ligand, and nH the Hill coefficient. Kinetic parameters were obtained by curve fitting of the data with KaleidaGraph. An apparently biphasic saturation curve for FBP of the mutant enzyme (see Fig. 4) was fitted using the following equation,

$$v = V_{min} + \frac{(V_{m,low} - V_{min})[FBP]}{S_{0.5,low} + [FBP]} + \frac{(V_{m,high} - V_{m,low} - V_{min})[FBP]}{S_{0.5,high+}[FBP]}$$

where V_{min} is the minimal reaction velocity without FBP, $V_{m,low}$ and $V_{m,high}$ the maximal velocities with low and high concentration of FBP, respectively, $S_{0.5,low}$ and $S_{0.5,high}$ the half-saturating FBP concentrations with low and high concentration of FBP, respectively, and [FBP] the FBP concentration.

Results and discussion

FBP-Independent catalytic activity of Q5 mutant LCLDH

LCLDH exhibits a uniquely high pH-dependence for enzyme activation among known bacterial allosteric L-LDHs (*27–30*, *39–41*). Under acidic conditions (e.g. pH 5.0), LCLDH exhibits marked catalytic activity due to the homotropic activation effect of substrate pyruvate even in the absence of FBP, in which the enzyme shows a sigmoidal-shaped pyruvate saturation curve (Fig. 2). FBP greatly improves the catalytic reaction of the enzyme by changing the sigmoidal saturation curve into a hyperbolic one, which gives a greatly reduced half-saturating concentration ($S_{0.5}$) and a slightly increased V_m value for pyruvate. Under neutral conditions (e.g. pH 7.0), on the other hand, LCLDH exhibits virtually no catalytic activity unless FBP is present (Fig. 3A), and requires a much higher concentration of FBP (about 4×10^4-fold) for enzyme activation than at pH 5.0, although the activation function of FBP is more than 100-fold improved in the presence of certain divalent cations such as Mn^{2+} (Fig. 4A). Since the allosteric regulation of LCLDH thus highly depends on the pH, we compared the catalytic properties of the wild-type and Q5 mutant enzymes at both pH 5.0 and 7.0.

The Q5 mutant enzyme exhibited a hyperbolic saturation curve for pyruvate at pH 5.0 even in the absence of FBP, in which it exhibited an about 32-fold smaller $S_{0.5}$ for pyruvate and a 6-fold larger V_m than the wild-type enzyme (Fig. 2 and Table I). As compared with the fully activated wild-type enzyme with a saturation level (5 mM) of FBP, the mutant enzyme exhibited a slightly larger (less than twice) $S_{0.5}$ (K_m) value for substrate pyruvate and a significantly increased (about twice) V_m value, and thereby rather high catalytic efficiency ($V_m/S_{0.5}$ value) in the absence of FBP. In the presence of 5 mM FBP, on the other hand, the mutant enzyme exhibited slightly reduced $S_{0.5}$ (K_m) and V_m values for pyruvate, by 2.4 and 1.9-fold, respectively, and consequently exhibited an only 1.3-fold larger $V_{max}/S_{0.5}$ value than the values without FBP. The mutant enzyme thus exhibited virtually the equivalent $S_{0.5}$ and V_{max} values to those of the fully activated wild-type enzyme, and also LPLDH (*28*), independently of FBP, indicating that the LPLDH-like network induces essentially the complete activation of LCLDH at pH 5.0, through stabilization of the R state structure on allosteric equilibrium.

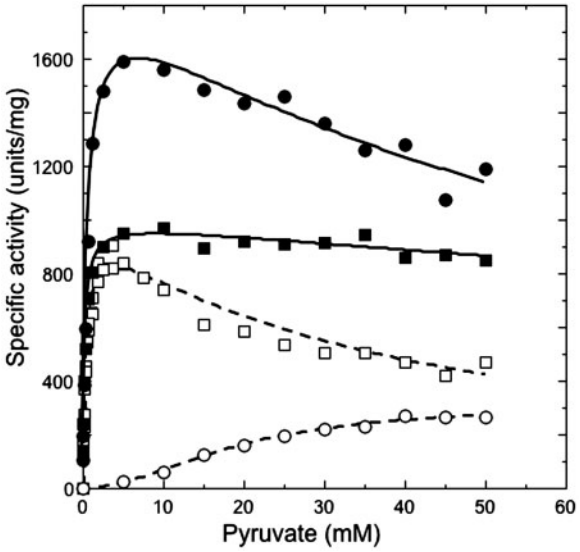

Fig. 2 Saturation curves for pyruvate of the wild-type and Q5 mutant LCLDHs at pH 5.0. The reaction velocities for the wild-type (open symbols) and Q5 mutant (closed symbols) LCLDH were measured in the presence of the indicated concentrations of pyruvate without (circles) and with (squares) 5 mM FBP. Dashed and solid lines indicate the calculated saturation curves for the wild-type and mutant enzymes, respectively, obtained with the kinetic parameters shown in Table I.

The mutant enzyme apparently exhibited lower substrate inhibition (larger K_i value) in the presence of FBP (Fig. 2 and Table I). It is known that L-LDH catalyses pyruvate reduction with NADH essentially through a compulsory ordered mechanism (*1*), and the substrate inhibition is thought to be a consequence of the formation of a covalent adduct between pyruvate and NAD^+, before NAD^+ is released from the enzyme (*42*) The substrate inhibition is therefore usually correlated with substrate K_m, but the mutant enzyme showed a markedly higher $K_I/S_{0.5}$ ratio (1,270) in the presence of FBP than the wild-type enzyme with FBP (106) and the mutant enzyme without FBP (122). This suggests that FBP enhances the release of NAD^+ from the enzyme or reduces the affinity of the enzyme-NAD^+ complex to pyruvate in the case of the mutant enzyme. Since Arg171 is in the same α2F helix as Arg173, which is one of the key residues for FBP binding, the binding of FBP may critically influence the catalytic site structure through minor structural change.

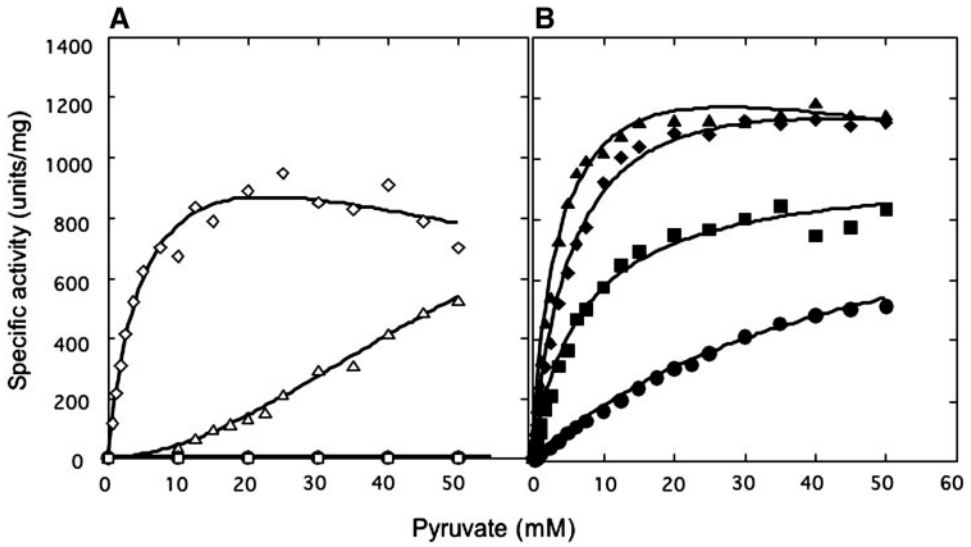

Fig. 3 Saturation curves for pyruvate of the wild-type (A) and Q5 mutant (B) LCLDHs at pH 7.0. The reaction velocities for the wild-type (open symbols) and Q5 mutant (closed symbols) LCLDH were measured in the presence of the indicated concentrations of pyruvate with no effector (circles), 10 mM $MnSO_4$ (squares), or 50 μM (for the mutant enzyme) or 5 mM (for the wild-type enzyme) FBP (triangles), and 10 mM $MnSO_4$, and 50 μM (for the mutant enzyme) or 5 mM (for the wild-type enzyme) FBP (diamonds). The lines indicate the calculated saturation curves for the wild-type and Q5 mutant enzymes, respectively, obtained with the kinetic parameters shown in Table I.

Table I. Kinetic parameters of the wild-type and Q5 mutant LCLDHs for substrate pyruvate[a].

	$S_{0.5}$ (mM)	V_{max} (U/mg)	$V_{max}/S_{0.5}$ (U/mg/mM)	K_I (mM)	n_H[b]
pH 5.0					
Wild-type					
None	20 (2)	310 (21)	15.5	nd[c]	2.0
+5 mM FBP	0.35 (0.04)	950 (30)	2,700	37 (4)	
Q5 mutant					
None	0.63 (0.05)	1,900 (50)	3,020	77 (8)	
+5 mM FBP	0.26 (0.02)	1,000 (20)	3,850	330 (60)	
pH 7.0					
Wild-type					
None	nd[c]	nd[c]	nd[c]	nd[c]	
+5 mM FBP	60 (20)	1,300 (490)	22	nd[c]	1.9
+10 mM Mn^{2+}	nd[c]	nd[c]	nd[c]	nd[c]	
+5 mM FBP + 10 mM Mn^{2+}	6.0 (1.3)	1,300 (150)	220	86 (31)	
Q5 mutant					
None	52 (4)	1,100 (50)	21	nd[c]	
+50 μM FBP	4.0 (0.3)	1,500 (50)	375	190 (40)	
+10 mM Mn^{2+}	7.2 (0.6)	970 (25)	135	nd[c]	
+50 μM FBP + 10 mM Mn^{2+}	6.1 (0.6)	1,440 (70)	236	310 (120)	

[a]Parameters were determined as described under the 'Materials and Methods' section, and standard deviations are shown in parentheses. [b]Hill coefficients (n_H) are shown only for the cases that exhibit significant cooperativity. [c]nd: reaction velocity is too low for determination of exact values.

Unlike the wild-type enzyme, the mutant enzyme exhibited marked catalytic activity also at pH 7.0 in the absence of FBP, showing a hyperbolic shaped pyruvate saturation curve (Fig. 3). In this case, however, the mutant enzyme exhibited a 8.7-fold larger $S_{0.5}$ (K_m) value and a slightly reduced V_{ma} value, and then a 10-fold lower $V_{max}/S_{0.5}$ value than the fully activated wild-type enzyme with 5 mM FBP and 10 mM Mn^{2+} (Table I). In addition, the reaction of the mutant enzyme was significantly enhanced with 50 μM FBP, which apparently saturated the mutant enzyme 80% (Fig. 4) mostly through reduction of the $S_{0.5}$ value for pyruvate, and then gave slightly higher catalytic efficiency ($V_{max}/S_{0.5}$) than for the fully activated wild-type enzyme (Fig. 3 and Table I). Figure 4 shows the dose-effects of FBP on the catalytic reactions of the two types of enzyme at pH 7.0 in the presence of 10 mM pyruvate. Unlike the case of the wild-type enzyme, FBP showed no apparent cooperative effect on the mutant enzyme, giving a 8,500-fold lower $S_{0.5}$ value than that of the wild-type enzyme. These results indicate that the LPLDH-like network greatly stabilized the R state structure of LCLDH on allosteric equilibrium also at pH 7.0.

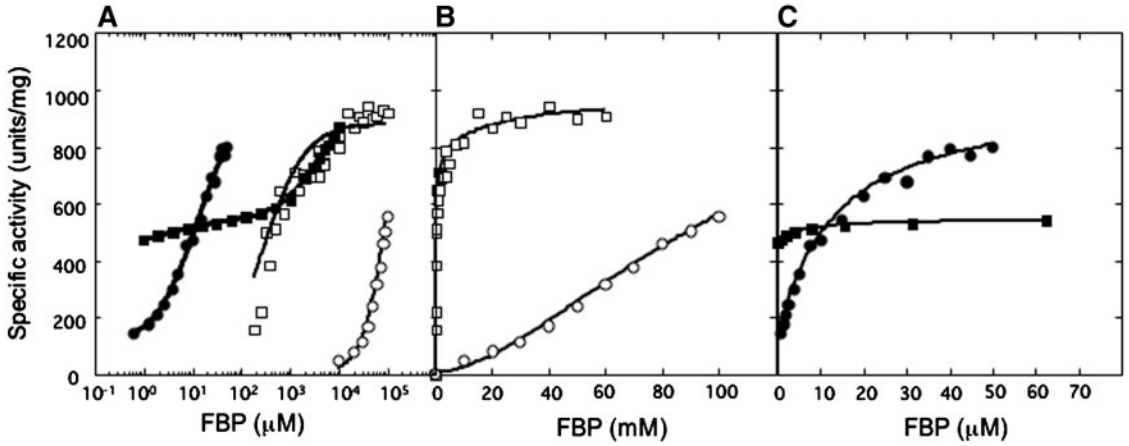

Fig. 4 Effects of FBP on the catalytic reactions of the wild-type and Q5 mutant LCLDHs at pH 7.0. The reaction velocities for the wild type (open symbols) and Q5 mutant (closed symbols) enzymes were measured in 50 mM sodium Mops buffer (pH 7.0) containing 0.1 mM NADH, 10 mM pyruvate and the indicated concentrations of FBP in the absence (circles) and presence (squares) of 10 mM $MnSO_4$. The lines indicate the calculated saturation curves obtained with the kinetic parameters shown in Table II. (A) The reaction velocities of the two enzymes plotted logarithmically as to the FBP concentration. (B) and (C) Linear plots of the reaction velocities of the wild-type and Q5 mutant enzymes, respectively, as to FBP concentration.

Effect of Mn^{2+} on the catalytic activity of Q5 mutant LCLDH

Some L-LDHs from lactic acid bacteria, such as *L. casei* and *L. curvatus*, constitute a subclass of bacterial allosteric L-LDHs that involve certain divalent metal ions such as Mn^{2+} in the allosteric regulation (*41*). In the case of LCLDH, Mn^{2+} ions exhibit no apparent activation effect on the enzyme reaction unless FBP is present, but greatly promote the activation function of FBP under neutral conditions through reduction of the $S_{0.5}$ value for FBP by more than 100-fold. It has been reported that LCLDH binds one Mn^{2+} ion per subunit in the absence of FBP, giving a dissociation constant of 0.26 mM at pH 7.0 (*25*). However, little is known at present as to how divalent cations are involved in the enzyme activity or activation function of FBP. Our efforts to crystallize the divalent metal-containing enzyme have not been successful, and the exact location of the binding site for divalent cations remains unclear, although SPR analysis and chemical modification for the enzyme suggested that the binding site is located in or near the FBP binding site (*24–26*). We evaluated the effects of Mn^{2+} on the catalytic properties of the Q5 mutant enzyme to gain more information on the involvement of Mn^{2+} in the allosteric regulation of LCLDH.

It is notable that Mn^{2+} significantly improved the reaction of the mutant enzyme in the absence of FBP, unlike in the case of the wild-type enzyme (Fig. 3 and Table I). The mutant enzyme exhibited an about 7-fold smaller K_m value for pyruvate and a slightly lower V_m value in the presence of 10 mM Mn^{2+}, in which the enzyme is sufficiently saturated with Mn^{2+} (Fig. 5B). However, Mn^{2+} ions (10 mM) exhibited an apparently lower activation effect on the enzyme than FBP (50 μM), which exhibited a 1.8-fold smaller pyruvate $S_{0.5}$ and a 1.5-fold higher V_m than Mn^{2+}, and rather inhibited the enzyme reaction in the presence of 50 μM FBP through an increase in the pyruvate $S_{0.5}$ and a reduction in the V_m value (Fig. 3 and Table I).

Figure 5 shows the dose-effects of Mn^{2+} on the reaction velocities of the two enzymes in the presence of 10 mM pyruvate. The mutant enzyme exhibited a slightly sigmoidal shaped saturation curve for Mn^{2+}, unlike in the case of saturation curve for FBP or substrate pyruvate. In addition, the mutant enzyme exhibited an apparent $S_{0.5}$ value of 0.8 mM for Mn^{2+}, which is comparable to the reported K_d for Mn^{2+} (0.26 mM) in the wild-type enzyme, indicating that both the T and R states of LCLDH can bind Mn^{2+} with essentially the same affinity, unlike in the case of FBP or pyruvate. It is therefore likely that Mn^{2+} stimulates the reaction of the mutant enzyme in a distinct manner from the T–R allosteric transition caused by FBP, possibly through induction of a minor structural change in the enzyme. On the other hand, Mn^{2+} reduced the catalytic efficiency of the mutant enzyme when the reaction mixture contained 50 μM FBP, but the inhibition curve of Mn^{2+} showed no apparent sigmoidal profile, the apparent half-inhibition concentration (IC_{50}) being 0.12 mM, indicating that FBP enhances the binding of Mn^{2+} in the mutant enzyme. It is noteworthy that the FBP saturation curve of the mutant enzyme showed an apparently biphasic profile, which is kinked around 10 μM FBP, in the presence of 10 mM Mn^{2+} (Fig. 4A, closed squares). Consequently, Mn^{2+} (10 mM) increased and decreased the reaction velocities of the mutant enzyme with below and above 10 μM FBP, respectively.

It has been reported that Mn^{2+} and FBP form a complex of 1 : 1 in ratio, the dissociation constant of which is only about 1 mM at pH 7.0 (*25*). This gives a simple explanation for the biphasic FBP saturation profile of the mutant enzyme with 10 mM Mn^{2+}. The mutant enzyme predominantly binds the FBP–Mn^{2+} complex with a low concentration of FBP, at which most FBP molecules exist as complexes, and increases the enzyme reaction through occupation of the binding site. Although the enzyme apparently exhibits 2.6-fold lower affinity to the free FBP molecule than the

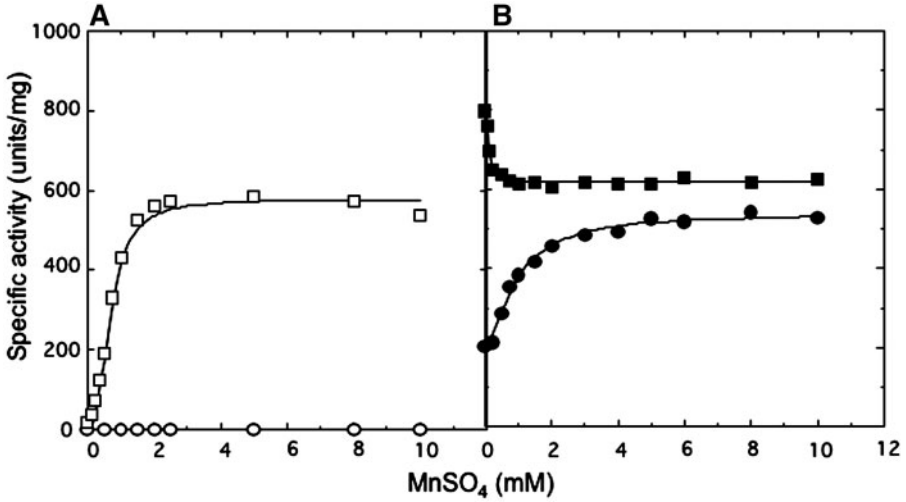

Fig. 5 Effects of $MnSO_4$ on the catalytic reactions of the wild-type (A) and Q5 mutant (B) LCLDHs at pH 7.0. The reaction velocities for the wild type (open symbols) and Q5 mutant (closed symbols) enzymes were measured in 50 mM sodium Mops buffer (pH 7.0) containing 0.1 mM NADH, 10 mM pyruvate and the indicated concentrations of $MnSO_4$ in the absence (circles) and presence (squares) of 50 μM (for the Q5 mutant enzyme) and 5 mM (for the wild-type enzyme) FBP. The lines indicate the calculated saturation curves obtained with the kinetic parameters shown in Table II.

complex (Fig. 4 and Table II), the enzyme replaces the complex with free FBP in the binding site with a high concentration of FBP, at which free FBP is more predominant than the complex, and thereby further increases the catalytic reaction. These features of the ligand binding likely approximate those of the R state of the wild-type LCLDH, i.e. the R state LCLDH exhibits higher affinity to the FBP–Mn^{2+} complex than free FBP, but the catalytic reaction is less improved with the complex than FBP alone.

The wild-type enzyme did not clearly show a biphasic FBP saturation curve in the presence of 10 mM Mn^{2+}, but showed a somewhat complicated saturation curve, which did not well fit to the simple Michaelis–Menten equation (Fig. 4A, open squares). Unlike the mutant enzyme, the wild-type enzyme requires the allosteric transition to the R state to gain the high affinity to the FBP–Mn^{2+} complex, and therefore requires a much higher concentration of FBP for activation by the complex. In the presence of a high concentration of FBP, the complex and free FBP coexist at comparable levels, and therefore compete with each other for the common binding site. These phenomena likely allow the wild-type enzyme to exhibit such a complicated FBP saturation curve with 10 mM Mn^{2+}.

Table II. Apparent kinetic parameters of the wild-type and Q5 mutant LCLDHs for FBP and Mn^{2+} at pH 7.0 in the presence of 10 mM pyruvate.

	$S_{0.5}$ (μM)	V_{min} (U/mg)[b]	V_{max} (U/mg)	n_H[c]
FBP				
no Mn^{2+}				
Wild-type	110,000 (3,000)	0	1,200 (100)	1.7
Q5 mutant	13 (2)	110 (20)	1,000 (50)	
+10 mM Mn^{2+}				
Wild-type	300 (50)	0	880 (20)	
Q5 mutant				
low conc.	5 (1)	460 (10)	540 (10)	
high conc.	4,600 (300)		1,000 (20)	
Mn^{2+}				
no FBP				
Wild-type	nd[d]	0	nd[d]	
Q5 mutant	800 (100)	190 (10)	540 (20)	1.5
+FBP				
Wild-type (5 mM)	640 (25)	0	580 (10)	2.4
Q5 mutant (50 μM)	120 (10)	620 (10)	800 (10)	2.1

[a]Parameters were determined as described under the 'Materials and Methods' section, and standard deviations are shown in parentheses. [b]V_{min}: minimal reaction velocity. [c]Hill coefficients (n_H) are shown only for the cases that exhibit significant cooperativity. [d]nd: reaction velocity is too low for determination of exact values.

Heat-stability of Q5 mutant LCLDH

Bacterial allosteric L-LDHs are usually stabilized toward denaturation in the presence of FBP except for the enzyme from *Enterococcus faecalis* (*43*), previously called *Streptococcus faecalis*, which is rather labile in the presence of FBP (*44*). In the case of non-allosteric LPLDH, on the other hand, the inter-subunit network may stabilize the enzyme instead of FBP, since it comprises six salt bridges (Fig. 1B) and thereby 24 salt bridges for the enzyme tetramer. We compared the heat-stabilities of the wild-type and Q5 mutant LCLDHs to determine the effects of the introduced inter-subunit salt bridges and the allosteric transition on the heat-stability.

Figure 6 shows the residual activities of the two types of LCLDH after heat treatment for 30 min at various temperatures. In the absence of FBP, the mutant enzyme exhibited a similar, or even lower, apparent denaturating temperature ($T_{1/2}$) than the wild-type enzyme in spite of the introduced salt bridge network, while it exhibited a markedly higher $T_{1/2}$ in the presence of 5 mM FBP (Fig. 6 and Table III), which is a saturating concentration for both types of

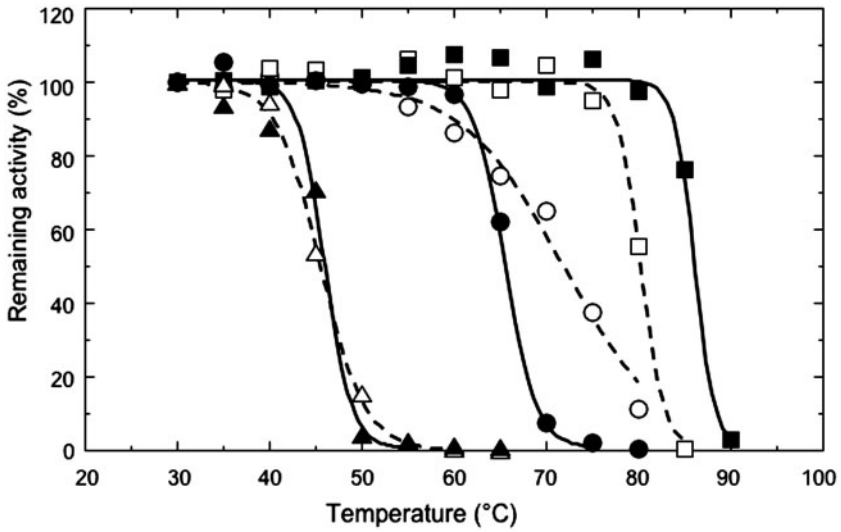

Fig. 6 Inactivation of the wild-type and Q5 mutant LCLDHs treated at various temperatures. The purified wild-type (open symbols) and Q5 mutant (closed symbols) enzymes were diluted to 1 μM with 100 mM sodium Mops buffer (pH 7.0) (triangles) or 100 mM sodium acetate buffer (pH 5.0) in the absence (circles) and presence (squares) of 5 mM FBP, and then treated for 30 min at the temperatures indicated.

enzyme at pH 5.0. In heat-stability, consequently, the mutant enzyme showed higher FBP-dependence than the wild-type enzyme, in contrast to in the case of catalytic activity. This result is nevertheless reasonable for the allosteric equilibrium of LCLDH, where the R state structure is intrinsically more labile than the T one, i.e. the allosteric constant (L) is 300 at pH 5.5, from which the change in Gibbs activation free energy of inactivation (ΔG) between the two state structures is estimated to be 3.4 kcal/mol (*30*). The salt bridge network likely increases the $T_{1/2}$ of the R state structure to be only equal to the level of the T state structure in the absence of FBP, in which the wild-type and mutant enzymes mostly form the T and R state structures, respectively. In contrast, the actual effect of the network on the heat-stability is clearly shown by the 7°C higher $T_{1/2}$ of the mutant enzyme in the presence of FBP, in which the two enzymes consistently form the R-state structure. The apparent higher FBP dependence of the mutant enzyme thus indicates that the R state structure is predominantly stabilized toward denaturation by FBP, as in the case of the allosteric equilibrium. On the other hand, the two enzymes consistently exhibited a markedly higher $T_{1/2}$ at pH 5.0 than pH 7.0 in the absence of FBP, indicating that LCLDH intrinsically exhibits great pH-dependence in the heat-stability, which is essentially independent of the T or R state structure.

Figure 7 shows the time-dependence of the heat-inactivation of the two enzymes. It is notable that the inactivation of the mutant enzyme apparently occurred more abruptly around the $T_{1/2}$ than that of the wild-type enzyme in the absence of FBP (Fig. 6). The heat-stabilities were therefore evaluated at two temperatures (45°C and 55°C, respectively) around the $T_{1/2}$ at pH 7.0 (Fig. 7B and C), at which the two enzymes exhibited apparently the same $T_{1/2}$ (46°C). In the absence of FBP, the mutant enzyme was inactivated more slowly at 45°C, but more rapidly at 55°C than the wild-type enzyme. Table III summarizes the thermodynamic parameters that were calculated from these data. The mutant enzyme exhibited greatly increased activation enthalpy of heat-inactivation ($\Delta H^{\ddagger}$) than the wild-type enzyme, giving a change in $\Delta H^{\ddagger}$ ($\Delta\Delta H^{\ddagger}$) of +38.9 kcal/mol. The increased $\Delta H^{\ddagger}$ compensates for the activation free energy of heat-inactivation ($\Delta G^{\ddagger}$) at the $T_{1/2}$ for the increased activation entropy ($\Delta S^{\ddagger}$), indicating that the two enzymes exhibit apparently the same $T_{1/2}$ in distinct manners. It is likely that the introduced LPLDH-like network is mostly responsible for the $\Delta\Delta H^{\ddagger}$. In the presence of FBP, on the other hand, the wild-type enzyme was also abruptly inactivated around the $T_{1/2}$ (80°C) at pH 5.0, as in the case of the mutant enzyme (Fig. 6). In this case, $\Delta H^{\ddagger}$ may be increased mostly through the multiple salt bridges between the bound FBP molecule and the enzyme (particularly Arg173 and His188).

At pH 5.0, the mutant enzyme lost the catalytic activity much more rapidly than the wild-type enzyme in the absence of FBP, but fully retained the activity for 60 min in the presence of 5 mM FBP, at which the wild-type enzyme lost more than 60% of the activity ($t_{1/2} = 44\,\text{min}^{-1}$), during heat treatment at 80°C (Fig. 7 A). At pH 7.0, the mutant enzyme was markedly protected from the heat-inactivation at 55°C by only a low concentration of FBP (50 μM), which exhibited no significant effect on the heat-stability of the wild-type enzyme, and consequently showed higher heat-stability than the wild-type enzyme (Fig. 7C). In the presence of 5 mM FBP, in addition, the mutant enzyme completely retained the enzyme activity in the treatment for 60 min, while the wild-type enzyme lost 50% of the activity. These results consistently indicate that the mutant enzyme is more greatly and sensitively affected by FBP in heat-stability than the wild-type enzyme. This is also consistent in the allosteric equilibrium of LCLDH, where the R state structure is predominantly

Table III. Heat-stabilities of the wild-type and Q5 mutant LCLDH and thermodynamic parameters in heat-denaturation of the two enzyme at pH 7.0 in the absence of allosteric effector.

	Wild-type	Q5 mutant
pH 5.0		
$T_{1/2}$[a] (°C)		
no FBP	72	66
+5 mM FBP	80	86
$t_{1/2}$[b] at 80°C (min)		
no FBP	11.8 (0.6)[c]	2.82 (0.10)[c]
+5 mM FBP	43.9 (5.5)[c]	nd[d]
pH 7.0		
$T_{1/2}$ (°C, no ligand)[a]	46	46
$t_{1/2}$ at 45°C (min, no ligand)[b]	35.5 (1.3)[c]	102.5 (7.2)[c]
$t_{1/2}$ at 55°C (min, no ligand)[b]	4.26 (0.07)[c]	1.88 (0.13)[c]
(+50 μM FBP)	4.41 (0.07)[c]	5.68 (0.18)[c]
(+5 mM FBP)	61.2 (2.2)[c]	nd[d]
(+10 mM Mn^{2+})	62.3 (2.4)[c]	52.1 (2.6)[c]
$\Delta G^{\ddagger}$ (kcal/mol) (45°C)[e]	24.9	25.6
$\Delta\Delta G^{\ddagger}$ (kcal/mol) (45°C)	0	+0.7
$\Delta G^{\ddagger}$ (kcal/mol)[e] (55°C)[e]	24.3	23.8
$\Delta\Delta G^{\ddagger}$ (kcal/mol) (55°C)	0	−0.5
$\Delta H^{\ddagger}$ (kcal/mol)[f]	43.3	82.2
$\Delta\Delta H^{\ddagger}$ (kcal/mol)[g]	0	+38.9
$\Delta\Delta S^{\ddagger}$ (kcal/mol/deg)[g]	0	+0.120

[a]$T_{1/2}$, the apparent half-denaturation temperature estimated from Fig. 6. [b]$t_{1/2}$, the apparent half-denaturation time, estimated from Fig. 7. [c]Values in parentheses indicate standard deviations in curve fitting of experimental data using Kleida Graph. [d]nd, the half-denaturating time is too long to be exactly determined. [e]$\Delta G^{\ddagger}$, the activation free energy of heat inactivation. $\Delta G^{\ddagger}$ was calculated with the absolute reaction rate equation (*61*), $\Delta G^{\ddagger} = RT[\ln(k_B T/h) - \ln(k)]$, where R is gas constant, T is the absolute temperature, k_B is Boltzman's constant, h is Plank's constant and k is the denaturation rate calculated from $t_{1/2}$. [f]$\Delta H^{\ddagger}$, the activation enthalpy of heat inactivation. $\Delta H^{\ddagger}$ was calculated from the slope $[-(T + \Delta H^{\ddagger}/R)]$ of Arrhenius plot [$\ln(k)$ vs $1/T$], and essentially the same value in 45 and 55°C. [g]$\Delta\Delta H^{\ddagger}$ and $\Delta\Delta S^{\ddagger}$, the differences in the activation enthalpy and entropy of heat inactivation, respectively. $\Delta\Delta S^{\ddagger}$ was calculated from the equation, $\Delta\Delta G^{\ddagger} = \Delta\Delta H^{\ddagger} - T\Delta\Delta S^{\ddagger}$.

stabilized by FBP because of its much higher affinity to FBP than the T state structure, and implies that LCLDH does not only regulate the catalytic activity but also modulates the protein stability as to denaturation through the allosteric equilibrium, using the intrinsically heat-stable T state structure and the specific stabilization effect of FBP on the R state structure, according to the surrounding FBP level.

Like the wild-type enzyme, the mutant enzyme was markedly protected from heat-inactivation at 55°C (pH 7.0) in the presence of 10 mM Mn^{2+}, at which it showed virtually the same heat-stability as that of the wild-type enzyme (Fig. 7C). This result is consistent with the fact that the two enzymes exhibit similar affinity to Mn^{2+}, and indicates that unlike FBP Mn^{2+} equally stabilizes the T state and R state structures against heat-inactivation. Like the wild-type enzyme, in addition, the mutant enzyme was synergically stabilized in the presence of both Mn^{2+} and FBP. In the presence of 10 mM Mn^{2+}, the mutant enzyme was completely protected from inactivation for 60 min with only 50 μM FBP, as the wild-type enzyme was with 5 mM FBP. This result is in good agreement with the fact that the mutant enzyme, i.e. the R state structure of LCLDH, exhibits higher affinity to the FBP–Mn^{2+} complex than free FBP or Mn^{2+}.

Molecular design for constitutively active bacterial L-LDHs

Until now, amino acid replacements concerning the allosteric regulation of L-LDHs have been mostly centred in the P-axis subunit interface area. This area contains the FBP-binding site, where two sets of conserved Arg173 and His188 play key roles in the regulation by FBP in two juxtaposed subunits of the P-axis related dimer through the formation of salt bridges with the phosphate groups of FBP. Since replacement of Arg173 or His188 induces not only desensitization to FBP but also partial activation of TCLDH (*9*, *10*, *12*) and BLLDH (*20*–*22*), the positively charged side chains of these residues appear to destabilize the closed conformation of the P-axis related dimer in the R state structure through static repulsion unless these residues are neutralized by FBP. Nevertheless, the replacement of Arg173 with Gln induces no significant enzyme activation in the cases of BSLDH (*14*) and LCLDH (unpublished results of ours). In the case of LCLDH, in addition, no marked activation is induced by modification of His188, alkylation with 6-bromopyruvate (*26*) or replacement with Asp (*27*). In the case of BSLDH, on the other hand, a constitutively active mutant enzyme was obtained through directed evolution (*45*). Among the three replacements in the mutant enzyme, the Q203L replacement is likely responsible for the change in allosteric properties, since Gln203 is located at the P-axis subunit interface. Nevertheless, the crucial activation mechanism underlying the replacement remains uncertain, and the primary and secondary structures around position 203 are poorly conserved in other allosteric or non-allosteric L-LDHs.

Our study demonstrates a new molecular design, which likely introduces an LPLDH-like inter-subunit salt bridge network at the *Q*-axis subunit interface, for conversion of bacterial allosteric L-LDHs to constitutively active enzymes. The Q5 mutant LCLDH was crystallized by the same crystallization condition to that for the R-state structure of the wild-type enzyme (*30*), and preliminary X-ray analysis for the crystal indicated that the mutant enzyme in the crystal forms essentially the same overall structure to the R state of the wild-type enzyme, giving 0.27 Å of the deviation (RMSD value) for all Cα atoms of tetramer (data not shown). It is likely that the flexibility of Arg171, i.e. the α2F-αC(Q) contact area, is ubiquitously pivotal for the allosteric motion of allosteric L-LDHs, because the side chain of Arg171 is consistently flipped out from the active site in the inactive dimer of BSLDH (*18*) and the T state tetramer of BLLDH (*20*), as in the case of the T state of LCLDH (*30*). Since Arg171 is directly involved and centred in the salt bridge network, the network appears to be one of the keys for the functional divergence of bacterial L-LDHs during evolution, and the new design is likely available for many allosteric L-LDHs to enhance their FBP-independent activity.

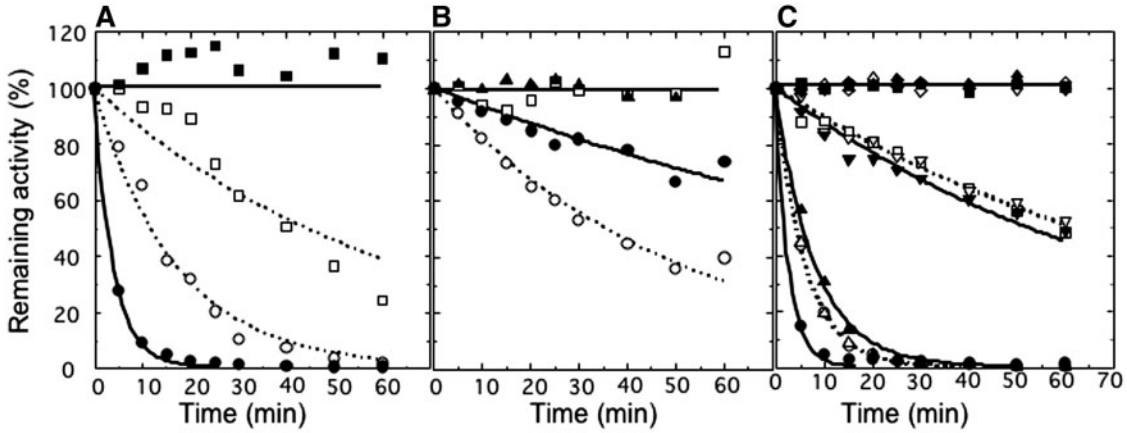

Fig. 7 Time-dependent heat-inactivation of the wild-type and Q5 mutant enzymes. The wild-type (open symbols) and Q5 mutant (closed symbols) enzymes were diluted to 1 μM with 100 mM sodium acetate buffer (pH 5.0) (A) or 100 mM sodium Mops buffer (pH 7.0) (B and C), and then treated at 80°C (A), 45°C (B), and 55°C (C) for the indicated time. Each heat treatment of the enzymes was performed with no ligand (circles), 50 μM FBP (triangles), 5 mM FBP (squares), 10 mM $MnCl_2$ (inverted triangles), or 10 mM $MnCl_2$ and 50 μM (for the Q5 mutant enzyme) or 5 mM (for the wild-type enzyme) FBP (diamonds). The dashed and solid lines indicate the calculated inactivation curves for the wild-type and Q5 mutant enzymes, respectively, obtained with the $t_{1/2}$ values shown in Table III.

Figure 8A shows the amino acid alignments for the αC, α2F and α2G helices of representative L-LDHs and L-malate dehydrogenase (L-MDH), together with the amino acids corresponding to His188. The five structure-known allosteric L-LDHs, i.e. LCLDH (*30*), BSLDH (*17*), BLLDH (*20*), TCLDH, which has the same amino acid sequence as structure-known *Thermus thermophilus* L-LDH (*46*) except for the residue at position 154, and *Thermotoga maritina* L-LDH (TMLDH) (*47*) consistently lack the LPLDH-like network at the *Q*-axis subunit interface, at which the relevant amino acids are completely missing except for the essential Arg171. In contrast, the relevant amino acids are fully conserved in the L-LDHs of *Pediococcus acidilactici* (PALDH) (*48*) and *Mycoplasma hyopneumoniae* (MHLDH) (*49*), in the latter of which only Lys235 is replaced with Arg, another basic amino acid. PALDH is known as an FBP-independent enzyme (*48*), and MHLDH is also considered to be an FBP-independent enzyme since it lacks both Arg173 and His188, although its crucial catalytic properties have not been reported (*49*). Although the 3D structures of the two enzymes remain unknown, these facts strongly suggest that the two enzymes employ the LPLDH-like network to exhibit their FBP-independent catalytic activity. Bacterial FBP-independent L-LDHs frequently lack Arg173 or His188, or both, as in the cases of LPLDH, PALDH and MHLDH. In the case of LPLDH, replacement of Asp188 with His induces no FBP-dependency of its catalytic activity, but marked FBP-dependency of its heat-stability (*34*). The mutant LPLDH exhibits a lower $T_{1/2}$ without FBP but a higher $T_{1/2}$ with FBP than the wild-type enzyme. These characteristics of the mutant LPLDH are well consistent in those of the Q5 mutant LCLDH, and suggest that loss of Arg173 or His188 is important for these enzymes to gain the FBP-independent protein stability rather than the FBP-independent high catalytic activity.

In contrast to these bacterial non-allosteric L-LDHs, vertebrate L-LDHs such as the dogfish muscle enzyme (DFLDH) (*50*) lack the amino acid residues relevant to the LPLDH-like network completely, but instead possess similar residues to those of allosteric L-LDHs, together with conserved Arg173 and His188 in the anion binding site (Fig. 8A), suggesting that the vertebrate enzymes employ a distinct strategy to gain their constitutive enzyme activity. Unlike bacterial L-LDHs, the vertebrate enzymes have a unique sequence of ~20 amino acids at the N-terminal of the first β strand (βA) in the NAD-binding domain (*1*). This sequence is called the 'R-arm' because it extends to the R-axis related subunit and undergoes a large number of inter-subunit interactions (*1*, *51*). On the other hand, L-MDH exhibit high identity in secondary and tertiary structure and functional amino acid residues with L-LDHs, but usually have dimeric structures that correspond to the *Q*-axis dimers of L-LDHs. Since the R-arm is missing in vertebrate dimeric L-MDHs, it has been thought to be a key structure for the association of the two *Q*-axis dimers into a tetramer of L-LDHs during evolution (*1*, *52*). It is notable that vertebrate dimeric L-MDHs partially form an LPLDH-like inter-salt bridge network. In pig heart cytosol L-MDH (PGMDH) (*53*), for example, Glu67, Lys178 and Lys235 of LPLDH are replaced with Gln, Leu and Arg, respectively, and thereby the salt bridge between Lys178 and Glu67(Q) is missing and the one between Arg171 and Glu67(Q) is replaced by a non-ionic hydrogen bond between Arg171 and Gln67(Q) (Fig. 8B, left). Instead of Lys235, however, Arg235 forms bidentate ionic hydrogen bonds with Asp68, compensating for the salt bridge network. These facts imply that vertebrate L-MDHs and L-LDHs employed distinct strategies to gain their constitutive catalytic activities during evolution.

While a dimeric L-MDH from *Aquaspirilium arcticum* (AAMDH), a psychrophilic bacterium, has virtually the same inter-subunit network as that of PGMDH, the enzyme from *Thermus thermophilus* (TTMDH), an extremely thermophilic bacterium, has a further strong inter-subunit network, which

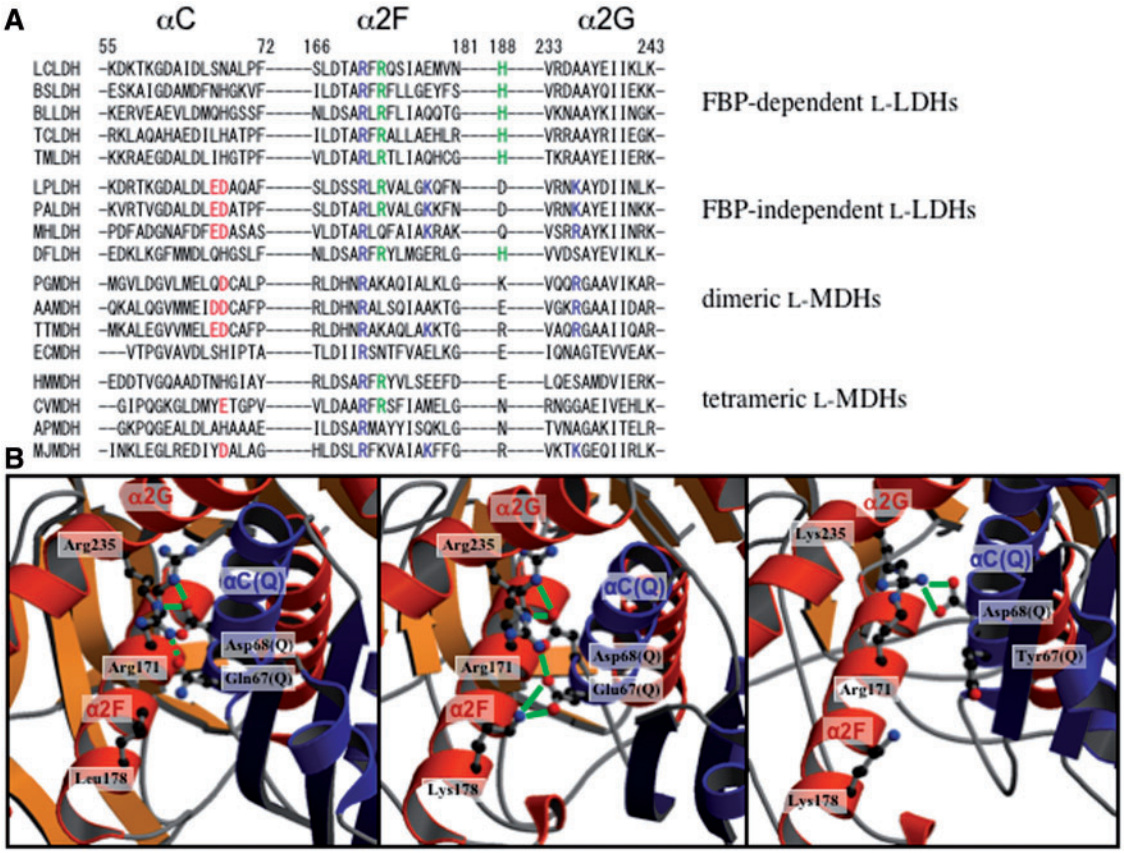

Fig. 8 Structural comparison of the αC, α2F and α2G (C-terminal half of the α1/2G helix) regions of representative L-LDHs and 3D structure-known L-malate dehydrogenases (L-MDHs). (A) Structure-based sequence alignment of L-LDHs and L-MDHs. Amino acid sequences were aligned for five FBP-dependent L-LDHs; *L. casei* (LCLDH) (*64*), *B. stearothermophilus* (BSLDH) (*65*), *B. longum* (BLLDH) (*66*), *Thermus caldophilus* (TCLDH) (*67*), and *Thermotoga maritima* (TMMDH) (*6*) L-LDHs, four FBP-independent L-LDHs; *L. pentosus* (LPLDH) (*68*), *Pediococcus acidilactici* (PALDH) (*48*), *Mycoplasma hyopneumoniae* (MHLDH) (1910283A) and dogfish muscle (DFLDH) (*50*) L-LDHs, four dimeric L-MDHs; *Sus scrofa* (pig heart, cytosol) (PGMDH) (PDB: 4MDH), *Aquaspirilium arcticum* (AAMDH (PDB: 1B8P)), *Thermus thermophilus* (TTMDH) (PDB:1IZ9), and *Escherichia coli* (ECMDH) (PDB: 2CMD), and four tetrameric L-MDHs; *Haloarcula marismortui* (HMMDH) (PDB: 1D3A), *Chlorobium vibrioforme* (CVMDH) (PDB: 1GV1), *Aerooyrum pernix* (APMDH) (PDB: 2D4A), and *Methanococcus jannaschii* (MJMDH) (PDB: 1HYG) L-MDHs. The residues of L-LDHs and L-MDHs are numbered according to the N-system for vertebrate L-LDHs proposed by Eventoff *et al.* (*69*). Acidic and basic amino acids relevant to the inter-subunit salt bridge network in LPLDH are shown in red and blue, respectively. Arg173 and His188 that are essential for the FBP binding are shown in green. (B) The *Q*-axis inter-subunit regions around Arg171 of three L-MDHs, PGMDH (left), TTMDH (middle), and MJMDH (right). The structures are represented by ribbon diagrams, where only the amino acids at positions 67, 68, 171, 178 and 235 are indicated by a ball and stick model. The two *Q*-axis-related subunits are coloured red and blue, as in Fig. 1. Salt bridges and hydrogen bonds among these amino acids are indicated by green solid and broken lines, respectively. The secondary structural elements of L-LDHs and L-MDHs are systematically named according to the names of the corresponding elements in vertebrate L-LDHs. The figures were drawn using MOLSCRIPT (*62*) and Raster3D (*63*).

comprises not only all the salt bridges of the LPLDH but also bidentate hydrogen bonds between Arg235 and Asp68 as in PGMDH and AAMDH (Fig. 8B, middle), in striking contrast to *Thermus* allosteric L-LDHs (*54*). Structural comparison thus strongly suggests that the LPLDH-like salt bridge network is widely used in constitutively active L-2-hydroxyacid dehydrogenases such as non-allosteric L-LDH and L-MDH.

Nevertheless, an LPLDH-like network is not evident in the case of *E. coli* L-MDH (ECMDH), where none of the relevant amino acids but Arg171 is conserved at the *Q*-axis interface (Fig. 8A), although ECMDH has a unique inter-subunit salt bridge between His68 and Glu238(Q) (*55*), instead of the Asp68-Lys235(Q) salt bridge of LPLDH. This suggests that the LPLDH-like network is not the only way that provides dimeric L-MDHs with active conformations. Furthermore, an LPLDH-like network is not evident in these tetrameric L-MDHs, which were recently found in some microorganisms including *Archaea* (*56*), although their regulation properties remain uncertain. The enzymes from *Haloarcula marismortui* (HMMDH) (*57*), *Aeropyrum pernix* (APMDH) (*58*) and *Chlorobium vibrioforme* (CVMDH) (*59*) lack an LPLDH-like network completely, although instead of Asp68(Q) Glu68(Q) forms a inter-subunit salt bridge with Arg171 in CVMDH (1GV1). On the other hand, the enzyme from *Methanococcus jannaschii* (MJMDH) (*60*), a hyperthermophilic archaeon, possesses the relevant residues except Glu67, which is replaced by Tyr. In the case of MJMDH, nevertheless, the relative positions of the α2F, α3G and αC(Q) helices are significantly different from those in L-LDHs or dimeric L-MDHs, and thereby Asp68(Q) forms no apparent inter-subunit salt bridge with Lys235, but instead

exhibits bidentate hydrogen bonds with Arg171 (Fig. 8B, right), unlike in the case of LPLDH.

Conclusion

Introduction of an LPLDH-like inter-subunit salt bridge network drastically increases the FBP-independent catalytic activity in LCLDH, although it does not completely abolish the activation effect of FBP or Mn^{2+} under neutral conditions. Unlike for the catalytic activity, the network rather enhances the FBP-dependence of the heat-stability of the enzyme by markedly raising the $T_{1/2}$ and rather reducing the $T_{1/2}$ in the presence and absence of FBP, respectively, indicating that the R state structure is intrinsically more heat-labile than the T state structure, but predominantly stabilized by FBP. Bacterial allosteric L-LDHs thus likely modulate both their catalytic activity and protein stability as to denaturation through the allosteric equilibrium, using the intrinsically stable T state structure and the predominant stabilization effect of FBP on the R state structure. The introduced network markedly increases the activation enthalpy of enzyme inactivation ($\Delta H^{\ddagger}$), which compensates for the activation free energy ($\Delta G^{\ddagger}$) for increased activation entropy ($\Delta S^{\ddagger}$) at the $T_{1/2}$ in the absence of FBP. An LPLDH-like network is used in many constitutively active L-2-hydroxyacid dehydrogenases, and thus appears to be one of the keys for bacterial L-LDHs to gain constitutive catalytic activity during evolution, although it is not the only way. The molecular design involving the network is likely available for many bacterial allosteric L-LDHs to allow them to exhibit high catalytic activity independently of allosteric activators.

Conflict of interest
None declared.

References

1. Holbrook, J.J., Liljas, A., Steindel, S.J., and Rossmann, M.G. (1975) Lactate dehydrogenase in *The Enzymes* (Boyer, P.D., ed.) Vol. 11, 3rd edn, pp. 191–292, Academic Press, New York
2. Garvie, E.I. (1980) Bacterial lactate dehydrogenases. *Microbiol. Rev.* **44**, 106–139
3. Taguchi, H., Yamashita, M., Matsuzawa, H., and Ohta, T. (1982) Heat-stable and fructose 1,6-bisphosphate-activated L-lactate dehydrogenase from an extremely thermophilic bacterium. *J. Biochem.* **91**, 1345–1348
4. Machida, M., Matsuzawa, H., and Ohta, T. (1985) Fructose 1,6-bisphosphate-dependent L-lactate dehydrogenase from *Thermus aquaticuas* YT-1, an extreme thermophilile: activation by citrate and modification reagents and comparison with *Thermus caldophilus* GK24 L-lactate dehydrogenase. *J. Biochem.* **97**, 899–909
5. Tomita, T., Kuzuyama, T., and Nishiyama, M. (2006) Alteration of coenzyme specificity of lactate dehydrogenase from *Thermus thermophilus* by introducing the loop region of NADP(H)-dependent malate dehydrogenase. *Biosci. Biotechnol. Biochem.* **70**, 2230–2235
6. Wrba, A., Jaenicke, R., Huber, R., and Stetter, K.O. (1990) Lactate dehydrogenase from the extreme thermophile *Thermotoga maritima*. *Eur. J. Biochem.* **188**, 195–201
7. Schär, H.P. and Zuber, H. (1979) Structure and function of L-lactate dehydrogenases from thermophilic and mesophilic bacteria. ((I) Isolation and characterization of lactate dehydrogenases from thermophilic and mesophilic bacilli. *Hoppe-Seyler's Z. Physiol. Chem.* **360**, 795–807
8. Taguchi, H., Matsuzawa, H., and Ohta, T. (1984) L-Lactate dehydrogenase from *Thermus caldophilus* GK24, an extremely thermophilic bacterium. Desensitization to fructose 1,6-bisphosphate in the activated state by arginine-specific chemical modification and the N-terminal amino acid sequence. *Eur. J. Biochem.* **145**, 283–290
9. Matsuzawa, H., Machida, M., Kunai, K., Ito, Y., and Ohta, T. (1988) Identification of an allosteric site residue of a fructose 1,6-bisphosphate-dependemt L-lactate dehydrogenase of *Thermus caldophilus* GK24: production of a non-allosteric form by protein engineering. *FEBS Lett.* **233**, 375–378
10. Schröder, G., Matsuzawa, H., and Ohta, T. (1988) Involvement of the conserved histidine-188 residue in the L-lactate dehydrogenase from *Thermus caldophilus* GK24 in allosteric regulation by fructose 1,6-bisphosphate. *Biochem. Biophys. Res. Commun.* **152**, 1236–1241
11. Koide, S., Yokoyama, S., Matsuzawa, H., Miyazawa, T., and Ohta, T. (1991) Conformation of NAD^+ bound to allosteric L-lactate dehydrogenase activated by chemical modification. *J. Biol. Chem.* **264**, 8676–8679
12. Koide, S., Yokoyama, S., Matsuzawa, H., Miyazawa, T., and Ohta, T. (1992) Conformational equilibrium of an enzyme catalytic site in the allosteric transition. *Biochemistry* **31**, 5362–5368
13. Clarke, A.R., Atkinson, T., Campbell, J.W., and Holbrook, J.J. (1985) The assembly mechanism of the lactate dehydrogenase tetramer from *Bacillus stearothermophilus*; the equilibrium relationships between quaternary structure and the binding of fructose 1,6-biphosphate, NADH and oxamate. *Biochim. Biophys. Acta* **829**, 387–396
14. Clarke, A.R., Wigley, D.B., Barstow, D.A., Chia, W.N., Atkinson, T., and Holbrook, J.J. (1987) A single amino acid substitution deregulates a bacterial lactate dehydrogenase and stabilizes its tetrameric structure. *Biochim. Biophys. Acta* **913**, 72–80
15. Clarke, A.R., Atkinson, T., and Holbrook, J.J. (1989) From analysis to synthesis: new ligand binding sites on the lactate dehydrogenase framework. *Trends Biochem. Sci.* **14**, 101–105, 145–148
16. Piontek, K., Chakrabarti, P., Shär, H-P., Rossmann, M.G., and Zuber, H. (1990) Structure determination and refinement of *Bacillus stearothermophilus* lactate dehydrogense. *Proteins* **7**, 74–92
17. Wigley, D.B., Gamblin, S.J., Turkenburg, J.P., Dodson, E.J., Piontek, K., Muirhead, H., and Holbrook, J.J. (1992) Structure of a ternary complex of an allosteric lactate dehydrogenase from *Bacillus stearothermophilus* at 2.5 A resolution. *J. Mol. Biol.* **223**, 317–335
18. Cameron, A.D., Roper, D.I., Moreton, K.M., Mirhead, H., Holbrook, J.J., and Wigley, D.B. (1994) Allosteric activation in *Bacillus stearothermophilus* lactate dehydrogenase investigated by an X-ray crystallographic analysis of a mutant designed to prevent tetramerization of the enzyme. *J. Mol. Biol.* **238**, 615–625

19. Iwata, S. and Ohta, T. (1993) Molecular basis of allosteric activation of bacterial L-lactate dehydrogenase. *J. Mol. Biol.* **230**, 21–27
20. Iwata, S., Kamata, K., Minowa, T., and Ohta, T. (1994) T and R states in the crystals of bacterial L-lactate dehydrogenase reveal the mechanism for allosteric control. *Nat. Struct. Biol.* **1**, 176–185
21. Fushinobu, S., Kamata, K., Iwata, S., Sakai, H., Ohta, T., and Matsuzawa, H. (1996) Allosteric activation of L-lactate dehydrogenase analyzed by hybrid enzymes with effector-sensitive and -insensitive subunits. *J. Biol. Chem.* **271**, 25611–25616
22. Fushinobu, S., Ohta, T., and Matsuzawa, H. (1998) Homotropic activation via the subunit interaction and allosteric symmetry revealed on analysis of hybrid enzymes of L-lactate dehydrogenases. *J. Biol. Chem.* **273**, 2971–2976
23. Mayr, U., Hensel, R., and Kandler, O. (1980) Factors affecting the quaternary structure of the allosteric L-lactate dehydrogenase from *Lactobacillus casei* and *Lactobacillus curvatus* as investigated by hybridization and ultracentrifugation. *Eur. J. Biochem.* **110**, 527–538
24. Mayr, U., Hensel, R., Pruscha, H., and Kandler, O. (1981) Reconstitution of the allosteric L-lactate dehydrogenase from *Lactobacillus casei* investigated by hybridization, *Eur. J. Biochem.* **115**, 303–307
25. Mayr, U., Hensel, R., Deparade, M., Pauly, H.E., Pfleiderer, G., and Trommer, W.E. (1982) Structure-function relationship in the allosteric L-lactate dehydrogenases from *Lactobacillus casei* and *Lactobacillus curvatus*. *Eur. J. Biochem.* **126**, 549–558
26. Hensel, R., Mayr, U., and Woenckhause, C. (1983) Affinity labeling of the allosteric site of the L-lactate dehydrogenase of *Lactobacillus casei*. *Eur. J. Biochem.* **135**, 359–365
27. Taguchi, H. and Ohta, T. (1995) Role of histidine 188 in fructose 1,6-bisphosphate- and divalent cation-regulated L-Lactate dehydrogenase of *Lactobacillus casei*. *Biosci. Biotech. Biochem.* **59**, 451–458
28. Arai, K., Kamata, T., Uchikoba, H., Fushinobu, S., Matsuzawa, H., and Taguchi, H. (2001) Some *Lactobacillus* L-lactate dehydrogenases exhibit comparable catalytic activities for pyruvate and oxaloacetate. *J. Bacteriol.* **183**, 397–400
29. Arai, K., Hishida, A., Ishiyama, M., Kamata, T., Uchikoba, H., Fushinobu, S., Matsuzawa, H., and Taguchi, H. (2002) An absolute requirement of fructose 1,6-bisphosphate for *Lactobacillus casei* L-lactate dehydrogenase activity induced by a single amino acid substitution. *Protein Eng.* **15**, 35–41
30. Arai, K., Ishimitsu, T., Fushinobu, S., Uchikoba, H., Matsuzawa, H., and Taguchi, H. (2010) Active and inactive state structures of unliganded *Lactobacillus casei* allosteric L-lactate dehydrogenase. *Proteins* **78**, 681–694
31. Monod, J. and Wyman, J. (1965) Changeux J-P. On the nature of allosteric transitions: a plausible model. *J. Mol. Biol.* **12**, 88–118
32. Grau, U.M., Trommer, W. E., and Rossmann, M.G. (1981) Structure of the active ternary complex of pig heart lactate dehydrogenase with *S*-lac-NAD at 2.7 Å resolution. *J. Mol. Biol.* **151**, 289–307
33. Hart, K.W., Clarke, A.R., Wigley, D.B., Waldman, A.D.B., Chia, W.N., Barstow, D.A., Atkinson, T., Jones, J.B., and Holbrook, J.J. (1987) A strong carboxylate-arginine interaction is important in substrate orientation and recognition in lactate dehydrogenase. *Biochim. Biophys. Acta* **914**, 294–298
34. Taguchi, H. and Ohta, T. (1992) Unusual amino acid substitution in the anion-binding site of *Lactobacillus plantarum* non-allosteric L-lactate dehydrogenase. *Eur. J. Biochem.* **209**, 993–998
35. Uchikoba, H., Fushinobu, S., Wakagi, T., Konno, M., Taguchi, H., and Matsuzawa, H. (2002) Crystal structure of non-allosteric L-lactate dehydrogenase from *Lactobacillus pentosus* at 2.3 Å resolution: specific interactions as subunit interfaces. *Proteins* **46**, 206–214
36. Bradford, M.M. (1976) A rapid and sensitive method for the quantitation of microgram quantities of protein utilizing the principle of protein-dye binding. *Anal. Biochem.* **72**, 248–254
37. Eszes, C.M., Sessions, R.B., Clarke, A.R., Moreton, K.M., and Holbrook, J.J. (1996) Removal of substrate inhibition in a lactate dehydrogenase from human muscle by a single residue change. *FEBS Lett.* **399**, 193–197
38. Dixson, M. and Webb, E.C. (1979) *Enzymes*. pp. 400–402, Longman, London
39. Holland, R. and Pritchard, G.G. (1975) Regulation of the L-lactate dehydrogenase from *Lactobacillus casei* by fructose-1,6-bisphosphate and metal ions. *J. Bacteriol.* **121**, 777–784
40. Gordon, G.L. and Doelle, H.W. (1976) Purification, properties and immunological relationship of L(+)-lactate dehydrogenase from *Lactobacillus casei*. *Eur. J. Biochem.* **67**, 543–555
41. Hensel, R., Mayr, U., Stetter, K.O., and Kandler, O. (1977) Comparative studies of lactic acid dehydrogenases in lactic acid bacteria. 1. Purification and kinetics of the allosteric L-lactic acid dehydrogenases from *Lactobacillus casei ssp. casei* and *Lactobacillus curvatus*. *Arch. Microbiol.* **112**, 81–93
42. Gutfreund, H., Cantwell, R., and McMurray, C.H. (1968) The kinetics of the reversible inhibition of heart lactate dehydrogenase through the formation of the enzyme-oxidized nicotinamide-adenine dinucleotide-pyruvate compounds. *Biochem. J.* **106**, 683–687
43. Götz, F. and Schleifer, K.H. (1975) Purification and properties of a fructose 1,6-bisphosphate activated L-lactate dehydrogenase from *Staphylococcus epidermidis*. *Arch. Microbiol.* **105**, 303–312
44. Wittenberger, C. and Angelo, N. (1970) Purification and properties of a fructose-1,6-diphosphate-activated lactate dehydrogenase from *Streptococcus faecalis*. *J. Bacteriol.* **101**, 717–724
45. Allen, S.J. and Holbrook, J.J. (2000) Production of an activated form of *Bacillus stearothermophilus* L-2-hydroxyacid dehydrogenase by directed evolution. *Protein Eng.* **13**, 5–7
46. Coquelle, N., Fioravanti, E., Weik, M., Vellieux, F., and Madern, D. (2007) Activity, stability and structural studies of lactate dehydrogenases adapted to extreme thermal environments. *J. Mol. Biol.* **374**, 547–562
47. Auerbach, G., Ostendorp, R., Prade, L., Kornörfer, I., Dams, T., Huber, R., and Jaenicke, R. (1998) Lactate dehydrogenase from the hyperthermophilic bacterium *Thermotoga maritima*: the structure at 2.1 Å resolution reveal strategies for intrinsic protein stabilization. *Structure* **6**, 769–781
48. Garmyn, D., Ferain, T., Bernard, N., Hols, P., and Delcour, J. (1995) Cloning, nucleotide sequence, and transcriptional analysis of the *Pediococcus acidilacitici* L-(+)-lactate dehydrogenase gene. *Appl. Environ. Microbiol.* **61**, 266–272

49. Haldimann, A., Nicolet, J., and Frey, J. (1993) DNA sequence determination and biochemical analysis of the immunogenic protein P36, the lactate dehydrogenase (LDH) of *Mycoplasma hyopneumoniae*. *J. Gen. Microbiol.* **139**, 317–323
50. Taylor, S.S. (1977) Amino acid sequence of dogfish muscle lactate dehydrogenase. *J. Biol. Chem.* **252**, 1799–1806
51. Abad-Zapetero, C., Griffith, J.P., Sussman, J.L., and Rossmann, M.G. (1987) Refined crystal structure of dogfish M4 apo-lactate dehydrogenase. *J. Mol. Biol.* **198**, 445–467
52. Rossmann, M.G., Liljas, A., Brändén, C.-I., and Banaszak, L.J. (1975) *Evolutionary and structural relationship among dehydrogenases in The Enzymes* (Boyer, P.D., ed.) Vol. 11, 3rd edn, pp. 61–102, Academic Press, New York
53. Birktoft, J.J., Rhodes, G., and Banaszak, L.J. (1989) Refined crystal structure of cytoplasmic malate dehydrogenase at 2.5-A resolution. *Biochemistry* **28**, 6065–6081
54. Kim, S.Y., Hwang, K.Y., Kim, S.H., Sung, H.C., Han, Y.S., and Cho, Y. (1999) Structural basis for cold adaptation. Sequence, biochemical properties, and crystal structure of malate dehydrogenase from a psychrophile *Aquaspirillium arcticum*. *J. Biol. Chem.* **274**, 11761–11767
55. Hall, M.D., Levitt, D.G., and Banaszak, L.J. (1992) Crystal structure of *Escherichia coli* malate dehydrogenase. A complex of the apoenzyme and citrate at 1.87 A resolution. *J. Mol. Biol.* **226**, 867–882
56. Dym, O., Mevarech, M., and Sussman, J.L. (1995) Structural features that stabilize halophilic malate dehydrogenase from an archaebacterium. *Science* **267**, 1344–1346
57. Richard, S.B., Madern, D., Garcin, E., and Zaccai, G. (2000) Halophilic adaptation: novel solvent protein interactions observed in the 2.9 and 2.6 Angstroms resolution structures of the wild type and a mutant of malate dehydrogenase from *Haloarcula marismortui*. *Biochemistry* **39**, 992–1000
58. Kawakami, R., Sakuraba, H., Goda, S., Tsuge, H., and Ohshima, T. (2009) Refolding, characterization and crystal structure of (S)-malate dehydrogenase from the hyperthermophilic archaeon *Aeropyrum penix*. *Biochim. Biophys. Acta* **1794**, 1496–1504
59. Dalhus, B., Sarinen, M., Sauer, U.H., Eklund, P., Johansson, K., Karlsson, A., Ramaswamy, S., Bjork, A., Synstad, B., Naterstad, K., Sirevag, R., and Eklund, H. (2002) Structural basis for thermophilic protein stability: Structures of thermophilic and mesophilic malate dehydrogenases. *J. Mol. Biol.* **318**, 707–721
60. Lee, B.I., Chang, C., Cho, S.J., Eom, S.H., Kim, K.K., Yu, Y.G., and Suh, S.W. (2001) Crystal structure of the MJ0490 gene product of the hyperthermophilic archaebacterium *Methanococcus jannaschii*, a novel member of the lactate/malate family of dehydrogenases. *J. Mol. Biol.* **307**, 1351–1362
61. Eyring, H. and Stearn, A.E. (1939) The application of the theory of absolute reaction rates to proteins. *Chem. Rev.* **24**, 253–270
62. Kraulis, P.J. (1991) MOLSCRIPT: A program to produce both detailed and schematic plots of protein structures. *J. Appl. Cryst.* **24**, 946–950
63. Merritt, E.A. and Bacon, D.J. (1997) *Raster3D photorealistic molecular graphics in Methods in Enzymology* (Carter, C.W. Jr and Sweet, R.M., eds.) Vol. 277, pp. 505–524, Academic Press, New York
64. Kim, S.F., Baek, S.J., and Pack, M.Y. (1991) Cloning and nucleotide sequence of the *Lactobacillus casei* lactate dehydrogenase gene. *Appl. Environ. Microbiol.* **57**, 2413–2417
65. Barstow, D.A., Clarke, A.R., Chia, W.N., Wigley, D., Sharman, A.F., Holbrook, J.J., Atkinson, T., and Minton, N.P. (1986) Cloning, expression and complete nucleotide sequence of the *Bacillus stearothermophilus* L-lactate dehydrogenase gene. *Gene* **46**, 47–55
66. Minowa, T., Iwata, S., Sakai, H., Masaki, H., and Ohta, T. (1989) Sequence and characteristics of the *Bifidobacterium longum* gene encoding L-lactate dehydrogenase and the primary structure of the enzyme: a new feature of the allosteric site. *Gene* **85**, 161–168
67. Kunai, K., Machida, M., Matsuzawa, H., and Ohta, T. (1986) Nucleotide sequence and characteristics of the gene for L-lactate dehydrogenase of *Thermus caldophilus* GK24 and the deduced amino-acid sequence of the enzyme. *Eur. J. Biochem.* **160**, 433–440
68. Taguchi, H. and Ohta, T. (1991) D-lactate dehydrogenase is a member of the D-isomer-specific 2-hydroxyacid dehydrogenase family. Cloning, sequencing, and expression in *Escherichia coli* of the D-lactate dehydrogenase gene of *Lactobacillus plantarum*. *J. Biol. Chem.* **266**, 12588–12594
69. Eventoff, W., Rossmann, M.G., Taylor, S.S., Torff, H-J., Meyer, H., Keil, W., and Kiltz, H-H. (1977) Structural adaptations of lactate dehydrogenase isozymes. *Proc. Natl Acad. Sci. USA* **74**, 2677–2681